Theor Chem Acc (1999) 102:346–354
DOI 10.1007/s00214980m167

Theoretical Chemistry Accounts

Regular article

Generalized extended empirical bond-order dependent force fields including nonbond interactions*

Jianwei Che, Tahir Çağın, William A. Goddard III

Materials and Process Simulation Center, Beckman Institute (139-74), Division of Chemistry and Chemical Engineering, California Institute of Technology, Pasadena, CA 91125, USA

Received: 7 August 1998 / Accepted: 26 October 1998 / Published online: 16 March 1999

Abstract. We present a general approach for describing chemical processes (bond breaking and bond formation) in materials using force fields (FF) that properly describe multiple bonds at small distances while describing nonbond (Coulomb and van der Waals) interactions at long distances. This approach is referred to as the generalized extended empirical bond-order dependent FF. In this paper we use the Brenner empirical bond-order dependent FF for the short-range interactions and report applications on the energetics and structures of graphite crystal, dynamics of molecular crystals, and distortions of bucky tubes.

Key words: Nanotubes – Hydrocarbons – Molecular crystals – Structure – Mechanical properties

1 Introduction

For many important problems in the chemical and materials sciences, it is essential to describe the dissociation and formation of chemical bonds. Although high-quality quantum mechanical (QM) calculations can properly describe such reactive processes, many systems of interest are too large for QM calculations. Consequently, it is useful to have an accurate force field (FF) for molecular dynamics (MD) or Monte Carlo simulations of reactive systems. Standard FF are not adequate because they build specific bond orders into specific bonds and do not allow bond breaking [1, 2]. In contrast, a chemical reaction must allow bond orders to change during the dynamics. FF that do allow changes in bond order include the Tersoff FF [3, 4] for modeling phases of silicon and the Brenner bond order FF [5] (denoted Brenner FF) for simulating carbon and hydrocarbon systems [3–5]. The Brenner FF has been used for reactions of hydrocarbon species on diamond surfaces [6–11], fullerene molecules scattering on diamond surfaces [12], mechanical properties of graphite sheet and nanotubes [13, 14], atomic scale friction of diamond surfaces [15, 16], and the chemical vapor deposition of diamond films [5].

Despite its successes, the current form of the Brenner FF has limitations for accurate calculation of some material properties. For example, lone-pair electrons are not explicitly treated in the formulation, which leads to incorrect structures for radicals [5] such as CH_3. Also, the Brenner FF does not include the resonance effects of aromatics. However, the most serious limitation with the Brenner FF is that the long-range van der Waals and Coulomb interactions are not included explicitly. Such long-range interactions play an important role in molecular-based materials, including biological systems [17], bucky tubes, and self-assembly processes [18]. In order to simulate such systems, it is essential to include the long-range interactions systematically. Such a proper description of nonbond (NB) terms is required for interactions between molecules in a molecular crystal, between the bonded layers in a graphite crystal, and between bucky tubes. For these problems the Brenner FF is not adequate. To alleviate such problems Brenner et al. [19] suggested an ad hoc modification using a spline fit to connect various bond-order terms with long-range van der Waals interactions [19]. However, the position where the NB interaction should be switched on and off can lead to incorrect physical behavior when high pressure is applied since the NB forces between molecules or atoms might become too small in the spline region.

In this paper, we present the generalized extended empirical bond-order dependent (GEEBOD) FF which can be used with any bond-order dependent potential to properly describe any kind of NB interaction. GEEBOD is a consistent generalization of the Brenner approach and can be applied to more traditional FF with little modification.

In Sect. 2, we outline the original Brenner bond-order potential formulation, and present the GEEBOD approach of including NB interactions. Various numerical simulations are reported in Sect. 3 and the results are compared with the Brenner FF. Section 4 contains a summary.

* Contribution to the Kenichi Fukui Memorial Issue

Correspondence to: W.A. Goddard III

2 Theory

2.1 Formulation of the Brenner bond-order dependent FF

The Brenner bond-order dependent FF [5] sums over all pairs of atoms, with the total potential energy of a system given by [5]

$$V^{\mathrm{V}} = \sum_i \sum_{j>i} \left[V_{\mathrm{R}}(r_{ij}) - \bar{B}_{ij} V_{\mathrm{A}}(r_{ij}) \right] , \tag{1}$$

where V_{R} and V_{A} are the repulsive and attractive part of the pairwise binding potential, respectively. They are taken to have the form of a general Morse potential [5]

$$V_{\mathrm{R}}(r_{ij}) = f_{ij}(r_{ij}) \frac{D_{ij}^{\mathrm{e}} S_{ij}}{S_{ij} - 1} \exp\left[-\sqrt{2 S_{ij}} \beta_{ij} \left(r_{ij} - R_{ij}^{\mathrm{e}} \right) \right] \tag{2}$$

$$V_{\mathrm{A}}(r_{ij}) = f_{ij}(r_{ij}) \frac{D_{ij}^{\mathrm{e}} S_{ij}}{S_{ij} - 1} \exp\left[-\sqrt{\frac{2}{S_{ij}}} \beta_{ij} \left(r_{ij} - R_{ij}^{\mathrm{e}} \right) \right] , \tag{3}$$

where

$$f_{ij}(r) = \begin{cases} 1, & r \le R_{ij}^{(1)} \\ \left\{ 1 + \cos\left[\frac{\pi \left(r - R_{ij}^{(1)} \right)}{R_{ij}^{(2)} - R_{ij}^{(1)}} \right] \right\} / 2, & R_{ij}^{(1)} < r < R_{ij}^{(2)} \\ 0, & r \ge R_{ij}^{(2)} \end{cases} . \tag{4}$$

$f_{ij}(r)$ is a cutoff function that explicitly restricts the interaction to nearest neighbors. The bond-order parameter $\bar{B}_{ij}$ is written as [5]

$$\bar{B}_{ij} = \frac{B_{ij} + B_{ji}}{2} + F_{ij}\left(N_i^{\mathrm{H}}(t), N_j^{\mathrm{C}}(t), N_{ij}^{\mathrm{conj}} \right) . \tag{5}$$

Thus, $\bar{B}_{ij}$ depends on the environment around atoms i and j and implicitly contains many-body information. The values of the fitting parameters D_{ij}^{e}, S_{ij}, β_{ij}, and R_{ij}^{e}, etc., are given in Ref. [5].

As already mentioned, NB interactions are not considered in the Brenner FF. One approach to incorporate NB interactions is the switching-on method. When atoms fall into the NB region, NB interactions are turned on using a smooth function to combine the bond terms with NB terms [19]. Another method for including NB interactions is the partition method. We partition the system into distinct sets and calculate NB interactions between different sets (e.g., different layers in a graphite crystal) [14] but not within a set. Although such ad hoc modifications of the Brenner FF have been successful in solving specific problems, they are system-specific and are hard to generalize. For instance, the switching-on method cannot give the correct behavior for systems under high external loads. Under sufficiently high pressure, the distance between molecules will eventually be smaller than the turn-on point for NB interactions. This problem can be solved with the partition method but at the cost of preventing chemical reactions between atoms of different sets, reducing the advantage of bond-order dependent FF (as compared to traditional valence FF). It is also physically unreasonable to exclude NB interactions within each set since this neglects the terms responsible for steric interactions and it neglects the Coulomb interactions that surely exist within a set.

Next we present a consistent approach of implementing NB interactions in bond-order potentials which retains the reactive feature of bond-order potentials.

2.2 Inclusion of nonbond interactions

Physically, the chemical bond involves the overlap of partially occupied atomic orbitals on nearby atoms where high overlap leads to strong bonds [20]. The Pauli principle states that there are two electrons in a normal chemical bond. The interaction between orbitals of different bonds is very repulsive for short distances (Pauli principle) and attractive for larger distances (dispersion). The net effect is that NB interactions dominate at a much larger distance than do chemical bonding (valence) forces. Based on these considerations, we write the total potential energy of a system as follows

$$V^{\mathrm{tot}} = \sum_i \sum_{j>i} \left[V_{ij}^{\mathrm{V}} + P_{ij} V_{ij}^{\mathrm{NB}} \right] , \tag{6}$$

where V_{ij} and P_{ij} are functions of r_{ij}. The superscript V denotes the valence short-range terms (e.g., Brenner) and NB denotes the long-range NB terms. Here $P_{ij} = P_{ji}$ is a screening function that properly weights the NB contribution in the total energy. We take the form of the screening function to be

$$P_{ij} = f\left(V_{ij}^{\mathrm{V}}, V_{ij}^{\mathrm{V}} \right) \prod_{k \ne i,j} f\left(V_{ik}^{\mathrm{V}}, V_{kj}^{\mathrm{V}} \right) \tag{7}$$

with

$$f(x,y) = \begin{cases} \exp(-\gamma x^2 y^2) & \text{if } x < 0 \text{ and } y < 0 \\ 1 & \text{otherwise} \end{cases} . \tag{8}$$

Here γ is a scaling parameter; since the results presented here are not sensitive to the value of γ, we have used $\gamma = 1$.

The screening function eliminates NB interactions between two atoms i and j when they are directly bonded (i.e., $V_{ij}^{\mathrm{V}} < 0$) or when they are both bonded to a common atom k (i.e., $V_{ik}^{\mathrm{V}} < 0$ and $V_{kj}^{\mathrm{V}} < 0$). In both cases, the exponential function P_{ij} becomes negligibly small, and so NB interactions do not play a role. Thus, P_{ij} is a mathematical analog of the NB exclusion rules [1, 2] in traditional valence FF; however, Eq. (7) is more general and consistent. Unlike normal valence FF [1, 2], our formulation does not use molecular bond information. (We do implicitly use the convention that the strength of the bond goes to zero as the bond length goes to infinity, $V^{\mathrm{V}}(r_{ij} \to \infty) = 0$; our formulation could be modified to use a harmonic potential or other nondissociative potential to describe bonding.)

The force between atoms α and β is calculated from Eq. (6) through

$$F_{\alpha\beta} = -\frac{\partial V^{\mathrm{tot}}}{\partial r_{\alpha\beta}} , \tag{9}$$

where $F_{\alpha\beta} = F_{\alpha\beta}(r_{\alpha\beta})$. Substituting Eq. (6) into Eq. (9), leads to

$$F_{\alpha\beta} = \sum_i \sum_{j>i} \left\{ -\frac{\partial V_{ij}^{\mathrm{V}}}{\partial r_{\alpha\beta}} - f(V_{ij}^{\mathrm{V}}, V_{ij}^{\mathrm{V}}) \prod_{k\neq i,j} f(V_{ik}^{\mathrm{V}} V_{kj}^{\mathrm{V}}) \frac{\partial V_{ij}^{\mathrm{NB}}}{\partial r_{\alpha\beta}} \right.$$
$$- \frac{\partial f(V_{ij}^{\mathrm{V}}, V_{ij}^{\mathrm{V}})}{\partial r_{\alpha\beta}} \prod_{k\neq i,j} f\left(V_{ik}^{\mathrm{V}} V_{kj}^{\mathrm{V}}\right) V_{ij}^{\mathrm{NB}} - f\left(V_{ij}^{\mathrm{V}}, V_{ij}^{\mathrm{V}}\right)$$
$$\left. \times \sum_{k\neq i,j} \left[\frac{\partial f\left(V_{ik}^{\mathrm{V}}, V_{kj}^{\mathrm{V}}\right)}{\partial r_{\alpha\beta}} \prod_{k'\neq k,i,j} f(V_{ik'}^{\mathrm{V}}, V_{k'j}^{\mathrm{V}}) \right] V_{ij}^{\mathrm{NB}} \right\} . \tag{10}$$

Using the identity

$$\frac{\partial r_{ij}}{\partial r_{\alpha\beta}} = \delta_{ij,\alpha\beta} \tag{11}$$

leads to

$$F_{\alpha\beta} = F_{\alpha\beta}^{\mathrm{V}} + P_{\alpha\beta} F_{\alpha\beta}^{\mathrm{NB}}, -4\gamma \sum_{i>j} P_{ij} V_{ij}^{\mathrm{VDW}} (V_{ij}^{\mathrm{V}})^3 F_{ij,\alpha\beta}^{\mathrm{V}}$$
$$- \gamma \sum_{ijk} V_{ik}^{\mathrm{V}} V_{kj}^{\mathrm{V}} P_{ij} V_{ij}^{\mathrm{VDW}} (V_{ik}^{\mathrm{V}} F_{kj,\alpha\beta}^{\mathrm{V}} + V_{kj}^{\mathrm{V}} F_{ik,\alpha\beta}^{\mathrm{V}}) \tag{12}$$

where

$$F_{ij,\alpha\beta}^{\mathrm{V}} = -\frac{\partial V_{ij}^{\mathrm{V}}}{\partial r_{\alpha\beta}} , \tag{13}$$

$$F_{\alpha\beta}^{\mathrm{NB}} = \frac{\partial V_{\alpha\beta}^{\mathrm{NB}}}{\partial r_{\alpha\beta}} . \tag{14}$$

In Eq. (12) the first term $F_{\alpha\beta}^{\mathrm{V}}$ is from the valence FF term itself (e.g., Brenner). It represents the valence forces (i.e., bond stretching, bending, torsion, etc.). The remaining terms come from NB interactions and the screening function. Specifically, the second term represents the NB force between two properly screened atoms.

The third and fourth terms are the forces arising from correlations between screened bonds. In most cases, these contributions are negligible. Thus, if atoms i and j do not form a valence bond and do not form bonds with same atom k, then usually $F_{ij,\alpha\beta}^{\mathrm{V}} = 0$ and either $V_{ik}^{\mathrm{V}} = 0$ or $V_{kj}^{\mathrm{V}} = 0$, leading to zero contribution. On the other hand, if both atom i and j bind to a common atom or if they form a valence bond directly, these terms still have a negligible contribution because of the exponential screening factor P_{ij} because $V_{i\alpha}^{\mathrm{V}} < 0$ or $V_{i\beta}^{\mathrm{V}} < 0$.

The above formulation is quite general, applying to all kinds of NB interactions. For instance, V^{NB} can be van der Waals or Coulomb interaction or both. The form of the NB interaction does not alter the formulation. This approach provides a general method to incorporate NB interactions into the valence potential in a unified and continuous fashion. Therefore, it can be used not only in the bond-order dependent potential, but also in other more traditional valence FF with zero asymptotic limits.

We refer to the general approach described above as the (GEEBOD) FF. When the Brenner valence parameters are used for the valence terms, we refer this to as GEEBOD/BREN.

3 Sample applications

3.1 Hydrocarbon molecules

The Brenner FF gives good energetics and structures for most ground-state hydrocarbon molecules and radicals. For such small isolated molecules in the ground state, NB interactions are usually insignificant compared with binding energies. Since GEEBOD properly evaluates the contribution of NB interactions, we expect the new GEEBOD to retain the accuracy of the original Brenner FF for small isolated molecules. Indeed, Table 1 shows that the energetics and structures of small hydrocarbon molecules calculated from GEEBOD/BREN agree well with those from the original Brenner potential [5] and from experiment [5]. In these calculation we used a Lennard–Jones 12-6 description of the NB interactions

$$V_{ij}^{\mathrm{NB}} = \epsilon_0 \left[\left(\frac{\sigma}{r_{ij}}\right)^{12} - 2\left(\frac{\sigma}{r_{ij}}\right)^{6} \right] . \tag{15}$$

The parameters are listed in Table 2. Since the Brenner potential seems to account properly for NB interactions between H atoms [21], we did not include specific NB interactions involving H atoms (in general, we would include the terms to describe dissociative processes). Table 1 shows that GEEBOD/BREN achieves the same accuracy as the Brenner FF. This indicates that GEEBOD leads to the correct asymptotic behavior, where NB interactions are small. In this paper, we do not modify the valence FF terms in the Brenner FF. Therefore, known problems with the Brenner FF valence terms (resonance effects and inaccurate force constants) are not corrected.

Although NB interactions are insignificant for small isolated molecules, they can play a very important role in characterizing the properties of liquids and solids. In the subsequent sections, we will present results for three systems in which the NB interactions constitute a crucial source for their stability and mechanical properties.

3.2 Graphite crystal

Since the Brenner FF accounts for the conjugation within the graphite plane, it has been used to calculate properties of single graphite sheets and single-walled nanotubes (SWNT) [13, 22]. However, to calculate properties of graphite crystal, it is essential to also include long-range NB interactions. The graphite crystal has a layer separation [23] of 3.3545 Å at $T = 20°C$. With the Brenner FF, the interlayer interactions are zero because the layers are separated by much more than the near-neighbor cutoff (2.0 Å) in Brenner FF. Therefore, with the Brenner FF the energy of graphite crystal is independent of layer separation down to 2 Å. This leads to an infinite compressibility along the direction perpendicular to the graphite layers (until the interlayer separation is 2 Å).

Figure 1 shows the energetics of a graphite lattice as a function of interlayer separation (a measure of the compressibility). The dashed line is calculated from the

Brenner FF, while the solid curve is obtained from GEEBOD/BREN. The open circles in the figure are the values calculated from the GraFF [24] which gives accurate energetics, vibrational frequencies, and specific heat for graphite. GraFF serves as a standard to measure the accuracy of the results for graphite and nanotubes calculated from the original Brenner potential and the modified Brenner potential. We see that the Brenner FF leads to a flat potential curve until 2 Å because it does not have interlayer forces that oppose the deformation. With GEEBOD we obtain the same results as in GraFF for long ranges (~2 Å). While a graphite crystal is highly compressed, new valence bonds will form and phase transformation will occur, which results in a dramtic decrease in van der Waals energies. In Fig. 1, we do see this decrease in the GEEBOD potential curve. Note that GEEBOD does not partition the atoms into different groups (as in the partition method): all atoms are treated equally within each layer and across different layers. This is an unique feature of GEEBOD, which retains the bond-order dependence of the valence interactions while simultaneously incorporating NB interactions. Indeed, preliminary calculations using GEEBOD show that graphite transforms to diamond under high pressure. Such results cannot be obtained by the partition method.

In Fig. 2, we compare the power spectrum of a graphite lattice, to show the vibrational frequency. The spectrum shown here is the Fourier transformation of the velocity autocorrelation function

$$I(\omega) = \left| \int_{-\infty}^{\infty} \exp(-i\omega t)\langle V(t)V(0)\rangle dt \right|^2 . \qquad (16)$$

The solid line is calculated from GraFF, the dashed line is calculated from the GEEBOD potential, and the dotted line is obtained from the pure Brenner FF. The velocity auto-correlation functions are computed from fixed volume, fixed energy (NVE) MD starting with a graphite lattice at the average temperature of 300 K. As shown in Fig. 2, the Brenner FF does not account for the low-frequency modes corresponding to the shearing and breathing motion in the graphite lattice (which results from interlayer interactions). GEEBOD captures all these low-frequency lattice modes because the NB interactions are correctly built in. There are significant differences between GraFF and GEEBOD for various higher frequency modes. These modes correspond to

Table 1. Atomization energies (eV) for hydrocarbon molecules

Molecule	BrenFF	GEEBOD	Experiment
Methane	17.6	17.6	17.6
Ethane	29.7	29.7	29.7
Propane	42.0	42.0	42.0
n-Butane	54.3	54.3	54.3
i-Butane	54.3	54.3	54.4
n-Pentane	66.5	66.7	66.6
Isopentane	66.5	66.7	66.6
Neopentane	66.8	66.8	66.7
Cyclopropane	35.0	35.0	35.8
Cyclobutane	48.5	48.5	48.2
Cyclopentane	61.3	61.3	61.4
Cyclohexane	73.6	73.6	73.6
Ethylene	23.6	23.6	23.6
Propene	36.2	36.2	36.0
1-Butene	48.5	48.5	48.5
cis-Butene	48.9	48.9	48.6
Isobutene	48.4	48.4	48.7
$(CH_3)_2C{=}C(CH_3)_2$	73.3	73.2	73.4
Cyclopropene	27.3	27.3	28.8
Cyclobutene	42.0	42.0	42.4
Cyclopentene	55.7	55.7	55.6
1,4-Penradiene	55.0	55.0	54.8
$CH_2{=}CHCH{=}CH_2$	41.9	41.9	42.6
$CH_3CH{=}C{=}CH_2$	40.5	40.5	42.1
$H_2C{=}C{=}CH_2$	27.9	27.9	29.6
Acetylene	17.1	17.1	17.1
Propyne	29.4	29.4	29.7
1-Butyne	41.7	41.7	42.0
2-Butyne	41.7	41.7	42.2
Benzene	57.5	57.5	57.5
Toulene	69.6	69.6	70.1
1,4-Dimethylbenzene	81.8	81.8	82.6
Ethylbenzene	81.9	81.9	82.5
Ethenylbenzene	76.2	76.2	76.5
Ethynylbenzene	69.8	68.4	69.9
Naphthalene	91.4	91.4	91.2
CH_2	7.8	7.8	7.8
CH_3	12.7	12.7	12.7
$H_3C_2H_2$	25.7	25.7	25.5
H_2C_2H	18.9	18.9	18.9
C_2H	12.2	12.2	12.2
CH_2CCH	24.5	24.5	25.8
n-C_3H_7	38.0	38.0	37.8
i-C_3H_7	38.3	38.3	38.0
t-C_4H_9	50.5	50.5	50.5
Phenyl	52.7	52.7	52.7

Table 2. Lennard-Jones 12-6 parameters. The C—C van der Waals parameters come from the GraFF [21]. The H—H and C—H van der Waals parameters come from the Dreiding FF except that $\epsilon_{HH} = 0$

Type	C—C	C—H	H—H
ϵ_0 (kcal/mol)	0.0692	0.0324	0.0
σ (Å)	3.805	3.50	3.195

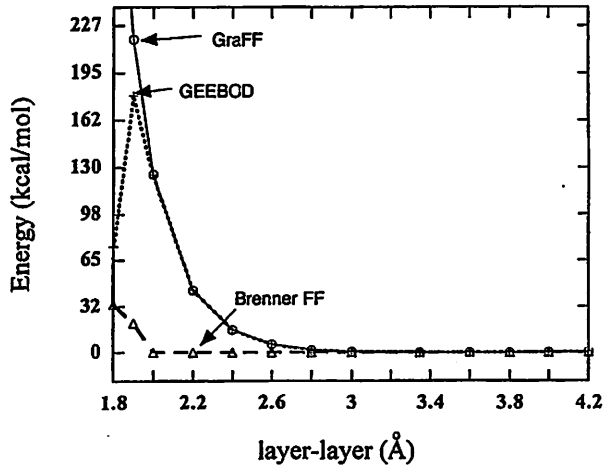

Fig. 1. The energy of a graphite lattice as a function of the distance ($C/2$) between two adjacent layers. The *open triangles* are from the Brenner FF, the *crosses* are from GEEBOD, and the *open circles* are from the GraFF

intralayer vibrations (bending, stretching), which are determined by the valence terms from Brenner FF. Comparison with GraFF (which gives accurate intralayer vibrational frequencies) shows that the Brenner FF is not accurate for the higher vibrational frequencies. Since GEEBOD builds in the NB interactions, it gives correct lattice stability and compressibility along the *c*-axis.

3.3 Molecular crystals

NB interactions are crucial in molecular crystals, self-assembled systems, and multi-walled nanotubes (MWNT). For molecular crystals, the intermolecular interactions are dominated by the van der Waals and Coulomb long-range interactions. Since the Brenner FF has no NB terms, molecules do not interact until they are very close (~2 Å). The Brenner FF cannot describe stable molecular crystals. As an example, we consider a naphthalene crystal at 300 K, where naphthalene is known to form a crystal. The experimental crystal structure of naphthalene is shown in Fig. 3 and we note that naphthalene molecules pack in a perfect ordered form with two orientations. Starting from the same crystal structure, we carried out 35 ps of MD (NVE) with an average temperature of 300 K using Brenner FF and GEEBOD. The simulation cell contained 192 naphthalene molecules, a 4 × 4 × 4 super cell, as shown in Fig. 3.

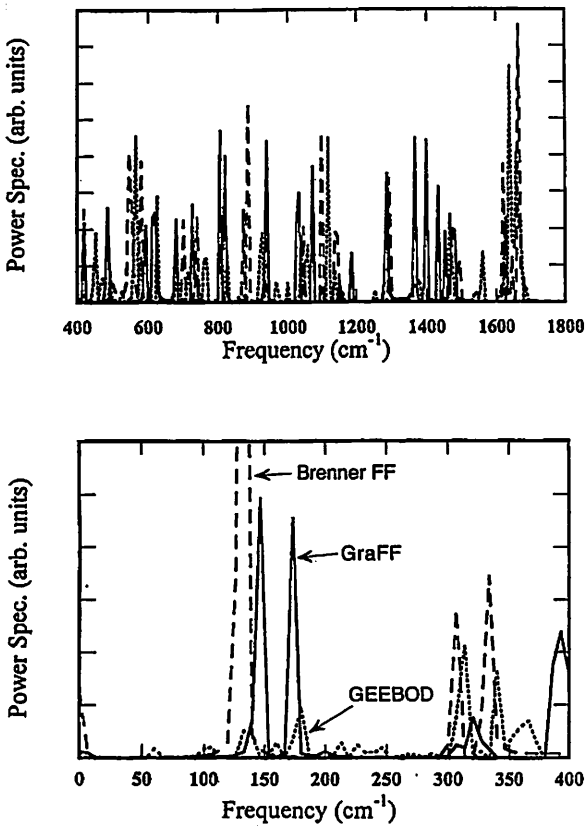

Fig. 2a,b. The power spectrum (vibrational frequency distribution) of graphite crystal. **a** High frequencies, **b** low frequencies. The *solid line* is calculated from GraFF, the *dashed line* is from the Brenner FF, and the *dotted line* is from GEEBOD

The radial distribution function (RDF) for the molecular center of mass is shown in Fig. 4. The solid line is the RDF of the starting structure, the dashed line is the RDF at the end of the simulation using GEEBOD, and the dotted line is the RDF at the final state using the Brenner FF. With GEEBOD we see that the crystal structure remains unchanged in the dynamics, with RDF peaks that broaden slightly due to the molecular thermal motion (Debye–Waller factor). However, the Brenner FF is not able to retain the crystal form of naphthalene. It leads to a step-function RDF as in a hard-sphere system.

To obtain more detailed structural information, we also calculated the distribution of molecular orientations. The angular distribution function (ADF) for a system in thermal equilibrium is defined as

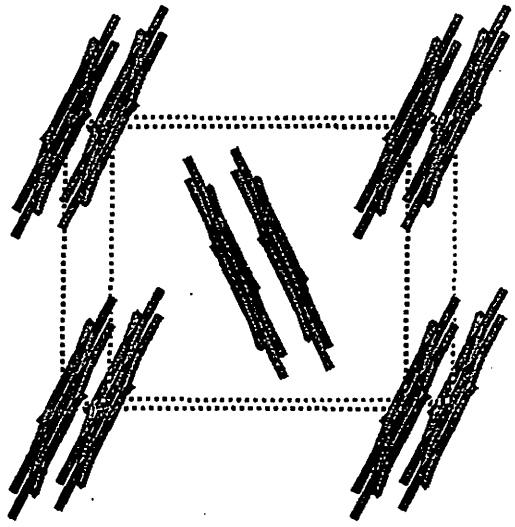

Fig. 3. One unit cell of the naphthalene molecular crystal. The unit cell parameters are, $a = 8.098$ Å, $b = 5.953$ Å, $c = 8.652$ Å, $\alpha = 90°$, $\beta = 124.4°$, and $\gamma = 90°$

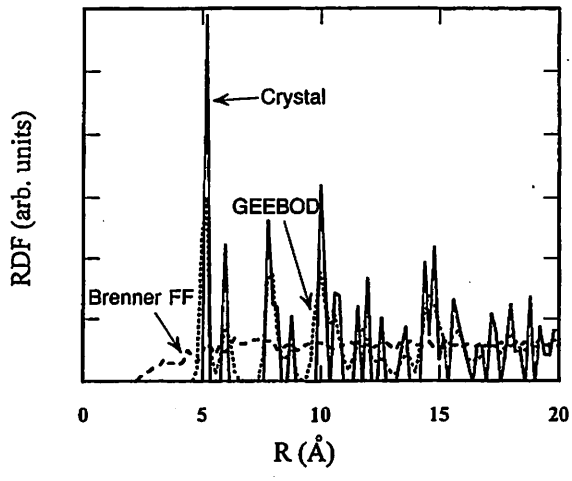

Fig. 4. The radial pair distribution function (*RDF*) of the molecular center of mass for naphthalene. The *solid line* is the RDF of the starting structure, the *dotted line* is the RDF at the end of the simulation using the modified potential, and the *dashed line* is the RDF at the final state using the pure Brenner potential

$$g(\hat{\mathbf{I}},\hat{\mathbf{I}}')=\sum_{i\neq j}\int_{v}\delta(\hat{\mathbf{I}}_i-\hat{\mathbf{I}})\delta(\hat{\mathbf{I}}_j-\hat{\mathbf{I}}')e^{-\beta V_{tot}}\,d^n v\Big/\int_{v}e^{-\beta V_{tot}}\,d^n v\ , \tag{17}$$

where the $\hat{\mathbf{I}}$ and $\hat{\mathbf{I}}'$ unit vectors represent the directions for the moment of inertia of two molecules. The angular distribution as a function of the angle between two vectors is calculated using

$$\rho(\cos\theta)=\int_{\hat{\mathbf{I}}\cdot\hat{\mathbf{I}}'=\cos\theta}\int g(\hat{\mathbf{I}},\hat{\mathbf{I}}')\,d\Omega\,d\Omega'\ , \tag{18}$$

which provides a measure of the correlation on the orientational order in the crystal between the naphthalene molecules.

The naphthalene molecule is a planar molecule, with three primary moments of inertia. Since naphthalene molecules have two distinct orientations in the crystal form, the distribution of each moment of inertia will have two sharp peaks for the crystal form. When the system becomes disordered, these peaks disappear and merge into a flat background, since no direction is more preferred. The ADFs of the three principle moments of inertia are shown in Fig. 5. Figure 5a shows the ADF of the starting structure, a perfect crystal from experiment. Here we see two dominant peaks in the angular distribution at angles of 50.58° and 0° for I_1, 56.98° and 0° for I_2, and 25.18° and 0° for I_3. The ADF of the final state from MD using GEEBOD is shown in Fig. 5c. This demonstrates that GEEBOD retains the crystal form at room temperature, with the expected peak broadening due to thermal motion. Here we note that the distribution of molecules with different orientation tends to spread faster than those with parallel orientation, giving rise to a peak at 0° larger than the ones at other angles. However, since the system has only two primary orientations, the area under each peak is approximately the same (the difference being of the order of $(1/n)$, where n is the number of molecules). The centers of peaks in the ADF shift a small amount from the experimental values. This may be due to Coulomb interactions not included in the current calculations.

The ADF of the final state obtained from 30 ps dynamics using the Brenner FF is depicted in Fig. 5b. In just a few hundred femtoseconds the Brenner FF gives a completely amorphous structure. Here we see a flat angular distribution indicating random distributions of molecular orientation. Thus, the Brenner FF is not adequate for studying molecular crystals.

These distribution functions show that NB interactions are essential to simulate molecular crystal systems.

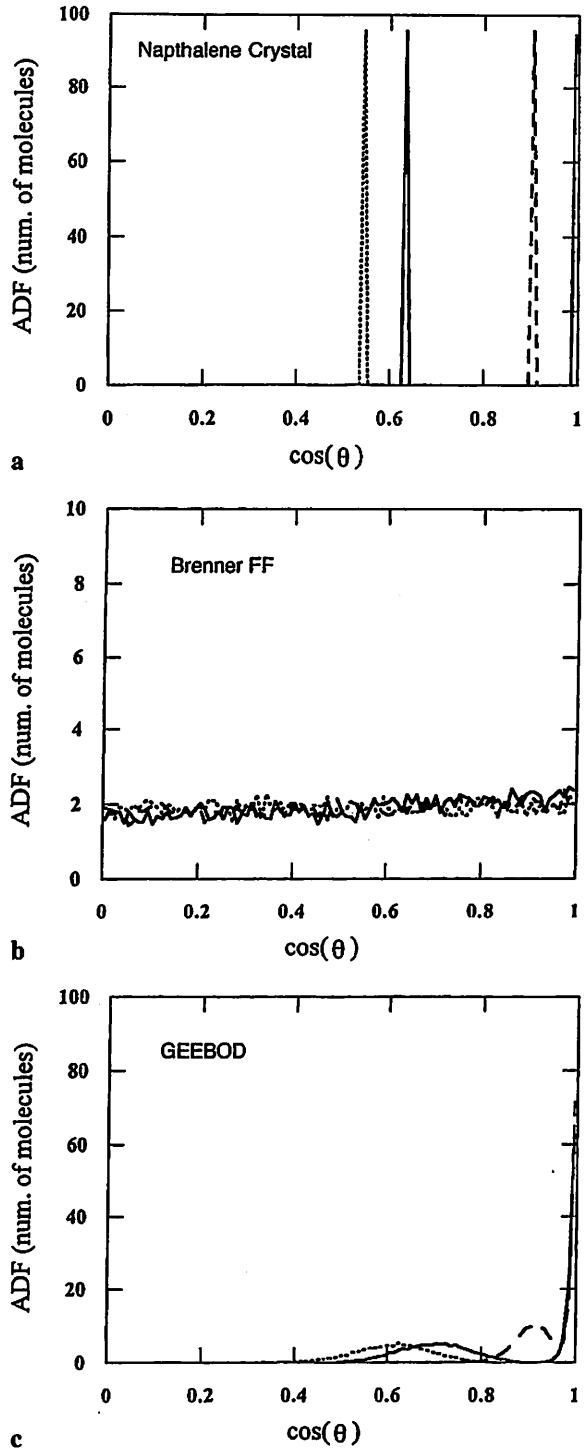

Fig. 5a–c. The angular distribution function (*ADF*) of the naphthalene molecules. a The angular distribution of three moments of inertia at the starting configuration (perfect crystal), b the moments of inertia angular distribution after 30 ps microcanonical dynamics at 300 K using the Brenner FF, and c the angular distributions of three principle moments of inertia after 30 ps dynamics using GEEBOD

3.4 Nanotubes

There is a great deal of interest in potential application of nanotubes, a new class of materials. Both calculations and experiment show that nanotubes are extremely strong [13, 25–29], with a strength of mass ratio approximately 100 times stronger than steel. Many researchers have used a variety of empirical potentials and approximate QM approaches to study the energetics and mechanical properties of nanotubes [13, 25, 26]. Since the Brenner FF does not include long-range interactions, it cannot be used to describe MWNT. This

would lead to the same problems as found for naphthalene. For instance, the bending modulus is greatly affected by the lack of NB interactions. The Brenner FF has been applied to SWNT [13], which are analogous to a single graphite sheet. Even for SWNT the NB interaction is crucial in nanotube ropes. Here one can use the partition method with the Brenner FF, using standard van der Waals potentials between different tubes while ignoring the NB interaction within each tube. This method can give the correct intertube interactions, but prevents the reaction between atoms in different tubes even where the tubes have broken ends.

The GEEBOD FF incorporates NB interactions in a more consistent and unified fashion so that all atoms are treated equivalently. In the following calculations, we demonstrate that GEEBOD treats the long-range interactions correctly. In each calculation, the zero of energy is chosen to be the ground-state energy of graphite.

3.4.1 Single-wall nanotubes

NB interactions can also be important for SWNT. Gao, et al. [30] demonstrated that for tubes less than 60 Å diameter the round SWNT is stable but that for larger tubes the most stable cross section has a dumbbell shape stabilized by van der Waals forces between the flat regions. As an example, Fig. 6 shows the energetics of a (70,70) nanotube for different conformations. To trace out the energies we applied constraints to restrict the distance between two atoms on opposite sides across the diameter of the nanotube. The energy is calculated from the optimal structure at each value of the constraint. The energies are plotted in Fig. 6 as a function of the constraint. The solid line is calculated from the GraFF, the dashed line is obtained from GEEBOD, and the dotted line is from the Brenner FF. We see that GEEBOD gives the correct energetic behavior, predicting that the collapsed form is energetically favored whereas the circular form is metastable. The Brenner FF cannot reproduce even the qualitative trend.

We also compared the energetics for nanotubes with various radii. Figure 7 shows the energetics for circular and collapsed nanotubes from (10,10) to (80,80). Figure 7a has the energetics for circular SWNT, while Fig. 7b shows the energetics of the collapsed form of SWNT. The energy per atom is relative to that of an atom in an isolated graphite sheet. For large radii, GEEBOD gives nearly the same result as GraFF: the small difference comes from the fact that the C—C bond length predicted by the Brenner bond terms is larger than that predicted by the valence FF. For large diameter nanotubes, most atoms are in the graphite sheet regions; therefore, the energetics differs from graphite only by the cohesive energy among the graphite layers. For nanotubes with small radii, the energetics is dominated by the strain energy. Thus, to predict the correct energetics requires accurate valence force constants. However, GEEBOD/BREN uses the Brenner FF valence force constants, which leads to inaccurate vibrational frequencies. This leads to discrepancies for small nanotubes. Nevertheless, these calculations show the importance of having correct NB interactions to calculate energetics and structures.

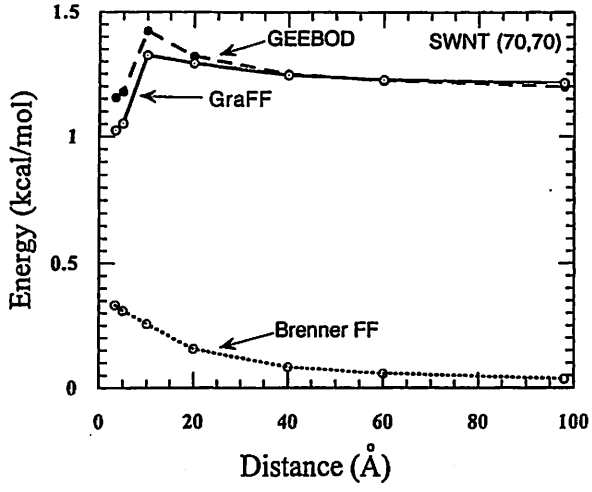

Fig. 6. The energetics of a (70,70) a single-walled nanotube (*SWNT*) as a function of the tube conformation. The *x*-axis is the constraint distance. The *solid line* is calculated from the valence force field, the *dashed line* is obtained from GEEBOD, and the *dotted line* is calculated from BrenFF

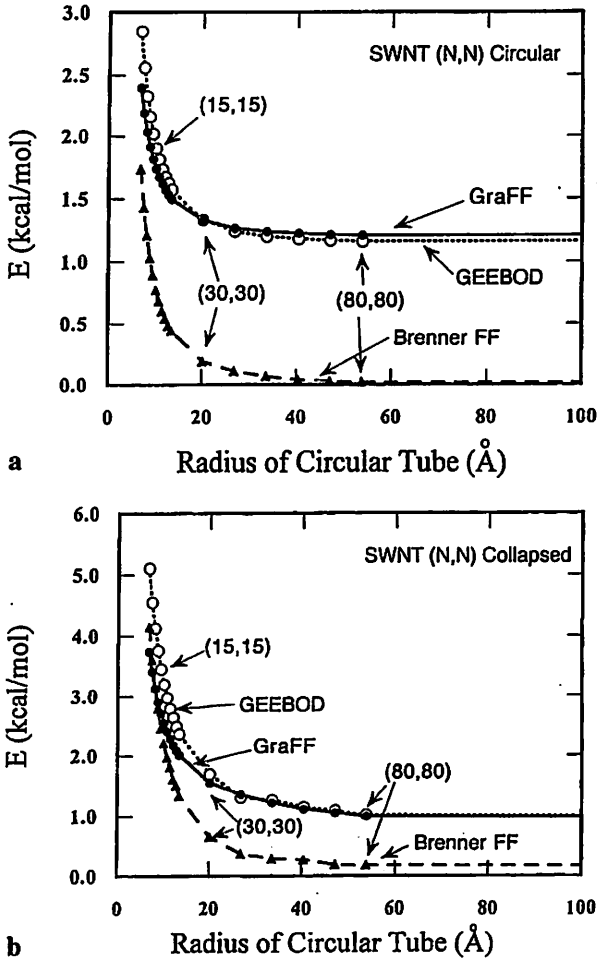

Fig. 7a,b. The energetics of SWNTs as a function of the tube size. **a** circular form of the nanotube, **b** collapsed form of the nanotube. The *solid line* is from GraFF, the *dotted line* is from GEEBOD, and the *dashed line* is calculated from BrenFF

Moreover, such NB interactions are essential in stabilize nanotube ropes (just as with molecular crystals).

3.4.2 Double-wall nanotubes

For MWNT, it is even more important to include NB interactions. As an example, we examined the bending behavior of a double-walled nanotube (DWNT) consisting of a (10,10) nanotube placed inside a (15,15) nanotube. The spacing between the walls is 3.48 Å, which is similar to the graphite interlayer separation (3.3545 Å). In this calculation, the tube is 20 layers long (containing 800 carbon atoms and 1200 carbon atoms, respectively).

We applied external forces perpendicular to the tube at both ends and in the opposite direction at the middle of the nanotube. The energy is computed from the optimal structures under various external loads. The sum of the external force is zero, and the torque is also zero. External forces are only applied to the outer tube atoms. On each end of the outer tube, 30 atoms experience the external load. At the middle of the outer tube 60 atoms suffer the force with the same magnitude but opposite direction. The energy of the DWNT as a function of the external force is shown in Fig. 8. The solid dots are for the Brenner FF while the open circles are computed from the GEEBOD. The lines give quadratic fits. These results show that the Brenner FF leads to a stiffness 28% too low for the DWNT. This is because the Brenner FF missed the extra resistance to deformation due to NB interactions between tubes.

For a continuous model, in the small deformation limit, the energy change for the DWNT can be written as

$$\Delta U = \frac{l^3 F^2}{6EI} \quad , \tag{19}$$

where E is the bending modulus, $l = 49.45$ Å is the length of the tube, I is the moment of inertia of the cross section, and F is the external force. Assuming a small deformation and a circular cross section, leads to

$$I = \frac{1}{4}\pi\left(R_{\text{out}}^4 - R_{\text{in}}^4\right) .$$

The radius of the (10,10) tube is calculated to be 6.98 Å, while the radius of the (15,15) tube is calculated to be 10.47 Å. Considering the spacing of planes in graphite to be 3.3545 Å we consider $R_{\text{out}} = 10.47 + 1.68 = 12.157$ Å and $R_{\text{in}} = 6.98 - 1.68 = 5.30$ Å. Substituting the results from Fig. 8 into Eq. (19) leads to $E = 944$ GPa for the GEEBOD FF. This compares with $E = 931$ GPa obtained from bending a SWNT (using the GraFF). The Brenner FF leads to $E = 740$ GPa which is 28% too low.

4 Conclusion

We have developped the (GEEBOD) FF to incorporate NB interactions into bond-order dependent potentials. GEEBOD recovers the results from the Brenner FF for systems when NB interactions are not important (small hydrocarbon molecules, diamond crystal). For systems

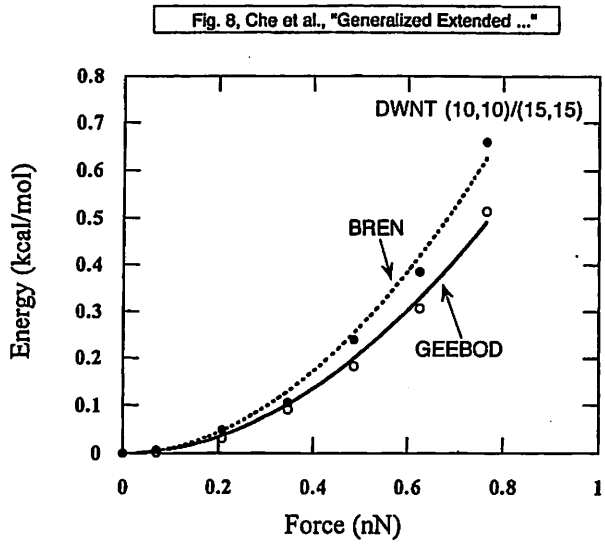

Fig. 8. The energetics of the double-walled nanotube (*DWNT*) [(10,10)/(15,15)] as a function of external load. The *open circles* are calculated from GEEBOD, and the *solid circles* are obtained using BrenFF. The *lines* are the quadratic fits for the two sets of calculations. The energy zero state is chosen to be the state without external force

where NB interactions are important, we demonstrate that GEEBOD can predict the correct physical behavior and properties. We did not consider examples with electrostatic interactions; however, these can be included without modifications.

In the applications described we used valence terms exactly as in the Brenner potential. GEEBOD does not alter the force constants in bond stretching and bending while extending the applicability of the Brenner FF to a much wider scope of applications.

GEEBOD can also be implemented with more general valence FF. Also GEEBOD can build more complete physics into the bond-order dependent potential. With such implementations, more complex biological and self-assembled systems can be studied.

Acknowledgements. We thank Guanhua Gao for helpful discussions. This research was funded by a grant from DOE-ASCI and by a grant from LLNL (C. Mailhoit). The facilities of the MSC are also supported by grants from NSF (ASC 92-17368 and CHE 91-12279), ARO (MURI), ARO (DURIP), ONR (DURIP), Chevron Petroleum Technology Co., Asahi Chemical, Owens-Corning, Exxon, Chevron Chemical Co., Asahi Glass, Chevron Research Technology Co., Avery Dennison, BP America, and the Beckman Institute.

Dedication. This paper is dedicated to Prof. Kenichi Fukui, a scholar, a gentlemen, and a ground-breaking scientist. Professor Fukui showed us how to use quantum mechanical reasoning to understand chemical reactivity. We will miss his insight and clarity of thought.

References

1. Rappé AK, Casewit CJ, Colwell KS, Goddard WA III, Skiff WM (1992) J Am Chem Soc 114: 10024
2. (a) Mayo SL, Olafson BD, Goddard WA III (1990) J Phys Chem 94: 8897; (b) Cornell WD, Cieplak P, Bayly CI, Merz

KM, Ferguson DM, Spellmeyer DC, Fox T, Caldwell JW, Kollman PA (1995) J Am Chem Soc 117: 5179; (c) Cornell WD, Cieplak P, Bayly CI, Merz KM, Ferguson DM, Spellmeyer DC, Fox T, Caldwell JW, Kollman PA (1996) J Am Chem Soc 118: 2309; (d) Weiner SJ, Kollman PA, Case DA, Chandra Singh U, Ghio C, Alagona G, Profeta S Jr, Weiner P (1984) J Am Chem Soc 106: 765; (e) Brooks BR, Bruccoleri RE, Olafson BD, States DJ, Swaminathan S, Karplus M (1983) J Comput Chem 4: 187; (f) Allinger NL, Yuh YH, Lii J-H (1989) J Am Chem Soc 111: 8551; (g) Mayo SL, Olafson BD, Goddard WA III, (1990) J Phys Chem 92: 7488

3. Tersoff J (1986) Phys Rev Lett 56: 632
4. Tersoff J (1988) Phys Rev B 37: 6991
5. Brenner DW (1990) Phys Rev B 42: 9458
6. Brenner DW, Robertson DH, Carty RJ, Srivastava D, Garrison BJ (1992) Mater Res Soc Symp Proc 278: 255
7. Garrison BJ, Dawnkaski EJ, Srivastava D, Brenner DW (1992) Science 255: 835
8. Alfonso DR, Ulloa SE, Brenner DW (1994) Phys Rev B 49:4948
9. Peploski J, Thompson DL, Rapp LM (1992) J Phys Chem 96: 8538
10. Chang X, Perry MD, Peploski J, Thompson DL, Rapp LM (1993) J Phys Chem 99: 4748
11. Perry MD, Rapp LM (1994) J Phys Chem 98: 4375
12. Mowrey RC, Brenner DW, Dunlap BI, Mintmire JW, White CT (1991) J Phys Chem 95: 7138
13. Robertson DH, Brenner DW, Mintmire JW (1992) Phys Rev B 45: 12592
14. Brenner DW, Harrison JA, White CT, Colton RJ (1991) Thin Solid Films 206: 220
15. Harrison JA, White CT, Colton RJ, Brenner DW (1993) J Phys Chem 97: 6573
16. Harrison JA, Brenner DW (1994) J Am Chem Soc 116: 10399
17. Vásquez M, Némethy G, Scheraga HA (1994) Chem Rev 94: 2183
18. Baremar JP, Cardini G, Klein ML (1988) Phys Rev Lett 60: 2152
19. Brenner DW, Robertson DH, Elert ML, White CT (1993) Phys Rev Lett 70: 2174
20. Wilson CW Jr, Goddard WA III (1972) Theor Chim Acta 26: 195
21. de P Sainte Claire, Song K, Hase WL, Brenner DW (1996) J Phys Chem 100: 1761
22. Omeltchenko A, Yu J, Kalia RK, Vashishta P (1997) Phys Rev Lett 78: 2148
23. Donohue J (1982) The structures of the elements. Krieger, Malaba Fla, p 256
24. Guo YJ, Karasawa N, Goddard WA III (1991) Nature 351: 464
25. Overney G, Zhong W, Tomanek D (1993) Z Phy D 27: 93
26. Yakobson BI, Brabec CJ, Bernholc J (1996) Phys Rev Lett 76: 2511
27. Ruoff RS, Tersoff J, Lorents DC, Subramoney S, Chan B (1993) Nature 364: 514
28. Treacy MMJ, Ebbesen TW, Gibson JM (1996) Nature 381: 678
29. Gao G (1998) Ph.D. thesis. California Institute of Technology
30. Gao G, Çağin T, Goddard WA III (1998) Nanotech 8: 183